Supporting material

Multiple-timescale Dynamics Underlying Spontaneous Oscillations of Saccular Hair Bundles

Yuttana Roongthumskul, Lea Fredrickson-Hemsing, Albert Kao, and

Dolores Bozovic

FIGURE S1: Mechanical model of a hair bundle

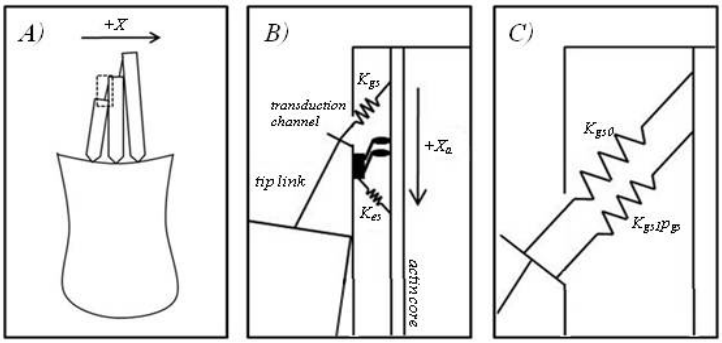

Fig. S1*A* shows a hair cell with a few of the 30-50 stereocilia that typically comprise a bundle. Horizontal displacement of the bundle is denoted by X, with positive direction chosen to be towards the tallest stereocilia. The transduction complex (*dashed box* in Fig S1*A*) is depicted in Fig S1*B*. Displacement of the myosin motors, denoted by X_a, is taken to be positive in the downward direction. While the transduction channels have been shown to be located at the lower end of the tip link in mammalian hair bundles (1), this location is not known in the amphibian counterpart. We arbitrarily depict the channel to be at the top end in the diagram but note that placing the channel at the lower end of the tip link would not significantly alter the model. The myosin motors are anchored to the insertional plaque near the transduction channel (*black rectangle* in the diagram). The variable gating spring with stiffness K_{gs} is illustrated in Fig S1*C*. The gating spring consists of two elastic elements in parallel, one of which has a calcium-dependent stiffness ($K_{gs1}p_{gs}$), while the stiffness of the other element is constant (K_{gs0}). The total stiffness of the combined springs (K_{gs}) is always positive.

Reference

1. Beurg M., R. Fettiplace, J.-H. Nam, and A. J. Ricci, 2009. Localization of inner hair cell mechanotransducer channels using high-speed calcium imaging. *Nat. Neurosci.* 12:553-558.

Table S1

Parameter	Definition	Fig 1B, 3B, 4-6, 8B, 9B	Fig 1C	Fig 2	Fig 3A	Fig 7B
r_m (nm)	Distance from the transduction channel to adaptation motor	20	100	20	20	20
N	Number of transduction channels			45		
γ	Geometrical gain of stereociliary shear motion			0.14		
d (nm)	Distance of gating spring relaxation on channel opening			7		
$p_{o,0}$	Resting open probability of transduction channels			0.5		
$k_{m,on}$(1/sM)	The rate of calcium binding to the adaptation motor	30×10^6	10×10^6	30×10^6	10×10^6	10×10^6
$k_{m,off}$ (1/s)	The rate of calcium unbinding from the adaptation motor	15×10^3	5×10^3	15×10^3	5×10^3	5×10^3
S_{max}(m/sN)	The maximal rate constant for slipping adaptation	640×10^3	800×10^3	800×10^3	550×10^3	400×10^3
S_{min} (m/sN)	The minimal rate constant for slipping adaptation			0		
C_{max} (m/s)	The maximal rate constant for climbing adaptation	0.058×10^{-6}	0.04×10^{-6}	0.058×10^{-6}	0.055×10^{-6}	0.02×10^{-6}
C_{min} (m/s)	The minimal rate constant for climbing adaptation			0		
X_{sp} (nm)	Resting deflection of stereociliary pivots	236	200	236	190	200
X_{es} (nm)	Resting deflection of extension spring	0	40	0	20	0
X_c (nm)	Resting extension of gating spring with channel closed	17	16	17	15	14
K_{es} (μN/m)	Stiffness of extent spring			140		
K_{sp} (μN/m)	Stiffness of stereociliary pivots	310	550	310	330	300
K_{gs0} (μN/m)	Stiffness of gating spring in the absence of calcium	2550	3000	2550	2200	2650
K_{gs1} (μN/m)	The slope of stiffness change with bound calcium	2000	2800	2000	1600	2100
$K_{gs,on}$ (1/sM)	The rate of calcium binding to the variable gating spring	30×10^6	60×10^6	30×10^6	30×10^6	5×10^6
$K_{gs,off}$ (1/s)	The rate of calcium unbinding from the variable gating spring	30	50	30	33	3.3

Table S1 Parameter values in simulations